

Searches for Higgs Bosons and Supersymmetry at the Tevatron

Volker Buscher

Physikalisches Institut, Universität Freiburg
Herrenberg-Str. 3, 79104 Freiburg, Germany

ABSTRACT

With almost 0.5 fb^{-1} of pp-collisions delivered in Tevatron Run II, both experiments CDF and DØ are reporting first results from a vast number of search analyses. This article summarizes the current status of Tevatron searches for Higgs bosons within the Standard Model and its extensions as well as direct searches for supersymmetric particles. Signatures for production of squarks, gluinos, charginos and neutralinos as predicted by gravity- and gauge-mediated SUSY breaking scenarios have been considered. No evidence for Higgs bosons or SUSY particles has been found so far. New limits are derived which significantly improve on existing limits.

1. Introduction

Since March 2001 the Tevatron pp-collider at the Fermi National Accelerator Laboratory is operating at a center-of-mass energy of 1.96 TeV and a bunch spacing of 396 ns (Run II). After an initial commissioning period for accelerator and detectors, the machine has delivered about 450 pb^{-1} between April 2002 and June 2004. Peak luminosities of up to $1.0 \cdot 10^{32} \text{ cm}^{-2} \text{ s}^{-1}$ have been achieved so far. Once the new recycler ring is fully operational the luminosity is expected to increase further, resulting in a projected Run II dataset of up to 8 fb^{-1} by the year 2009.

Given its high energy and steadily increasing luminosity, the Tevatron collider is an ideal tool for searches for massive particles beyond the reach of LEP. The results presented in this contribution are based on about 200 pb^{-1} of data recorded and analyzed by the two Tevatron experiments CDF and DØ. After a short description of the two detectors in Section 2, the status of searches for Higgs bosons and supersymmetric particles is summarized in Sections 3 and 4. For completeness, a brief overview of searches for other new physics is given in Section 5.

2. CDF and DØ Detectors

The CDF and DØ detectors are described in detail in Ref. [1] and [2]. Only a brief overview is presented in the following.

CDF track reconstruction relies on silicon detectors and a drift chamber situated inside a solenoid that provides a 1.4 T magnetic field coaxial with the beam. The silicon microstrip detector consists of eight cylindrical layers of mostly double-sided silicon, distributed in radius between 15 cm and 28 cm. The system is readout in about 700,000 channels and can provide 3D precision tracking up to pseudorapidities of 2.0. Outside of the silicon detectors and for pseudorapidities less than 1.0, charged particles are detected with up to 96 hits per track by the central outer tracker, an open-cell drift chamber with

alternating axial and 2 stereo superlayers with 12 wires each. Just inside the solenoid, a scintillator-based time-of-flight detector allows particle identification with a timing resolution of about 100 ps.

The electromagnetic (hadronic) calorimeters are lead-scintillator (iron-scintillator) sampling calorimeters, providing coverage up to pseudorapidities of 3.6 in a segmented projective tower geometry. Proportional wire and scintillating strip detectors situated at a depth corresponding to the electromagnetic shower maximum provide measurements of the transverse shower profile. In addition, an early energy sampling is obtained using preradiator chambers positioned between the solenoid coil and the inner face of the central calorimeter. Outside of the calorimeter and behind additional steel absorbers, a multi-layer system of drift chambers and scintillation counters allows detection of muons for pseudorapidities up to 1.5.

The tracking system of the D detector consists of a silicon vertex detector and a scintillating fiber tracker, situated inside a superconducting coil providing a 2 T magnetic field. The D silicon tracker has four cylindrical layers of mostly double-sided microstrip detectors covering 2.7 cm up to 9.4 cm in radius, interspersed with twelve disk detectors in the central region and four large disks in the forward region. The full system has about 800,000 channels and provides 3D precision tracking up to pseudorapidities of 3.0. The volume between the silicon tracker and the superconducting coil is instrumented with eight cylindrical double layers of scintillating fibers. Each layer has axial and stereo fibers (stereo angle $\approx 3^\circ$) with a diameter of 835 μm , that are readout using solid-state photodetectors (Visible Light Photon Counters, VLPCs).

The D calorimeter is a Liquid Argon sampling calorimeter with Uranium absorber (Copper and Steel for the outer hadronic layers) with hermetic coverage up to pseudorapidities of 4.2. Signals are readout in cells of projective towers with four electromagnetic, at least four hadronic layers and a transverse segmentation of 0.1 in both azimuth and pseudorapidity. The granularity is increased to 0.05 for the third EM layer, roughly corresponding to the electromagnetic shower maximum. To provide additional sampling of energy lost in dead material, scintillator-based detectors are placed in front of the calorimeter cryostats (preshower detectors) and between the cryostats (intercryostat detector). The preshower detectors consist of three layers of scintillator strips with VLPC readout providing, in addition to the energy measurement, a precise 3-dimensional position measurement for electromagnetic showers.

The D Muon system consists of three layers of drift tubes and scintillators, with toroid magnets situated between the first and second layer to allow for a stand-alone muon momentum measurement. Scintillator pixels are used for triggering and rejection of out-of-time backgrounds in both central and forward region. Proportional drift tubes are stacked in three or four decks per layer in the central region. Tracking of muons in the forward region is accomplished using decks of mini drift tubes in each layer, allowing muons to be reconstructed up to pseudorapidities of 2.0. The muon system is protected from beam-related backgrounds by shielding around the beam pipe using an iron-polyethylene-lead absorber.

Both CDF and D detectors are readout using a three-level trigger system which

reduces the event rate from 2.5 MHz to about 50 Hz. This includes programmable hardware triggers at Level 1 that provide basic track, lepton and jet reconstruction, secondary vertex or impact parameter triggers at Level 2 as well as a PC-based offline event reconstruction at Level 3.

3. Searches for Higgs Bosons

As the Run II luminosity increases, CDF and DØ will start reaching sensitivity to production of low-mass Higgs bosons beyond the LEP limits. For Standard Model Higgs bosons decaying to $b\bar{b}$, the production in association with W or Z bosons is the most promising channel. At masses up to about 180 GeV, Higgs bosons produced via gluon fusion might be observable in their decays to $W\bar{W}$. For models with more than one Higgs doublet, the coupling of the Higgs boson to b -quarks can be significantly enhanced, allowing to search for Higgs bosons produced in association with b -quarks.

The following sections summarize the current status and projections for the most important channels at Tevatron Run II.

3.1. Associated Production

The production of Higgs bosons in association with vector bosons can be searched for in all leptonic decays of W and Z : $W \rightarrow \ell \bar{\nu}$, $Z \rightarrow \ell \bar{\ell}$ and $Z \rightarrow \nu \bar{\nu}$ (with $\ell = e, \mu, \tau$). Sensitivity studies based on Monte Carlo simulation of detector performance throughout the course of Run II exist.[3,4] For WH production, first preliminary results[5] of searches in 162 pb^{-1} (CDF) and 174 pb^{-1} (DØ) of Run II data are described in the following.

Final states compatible with the WH signature can be selected by requiring one isolated lepton and missing transverse energy as well as two b -tagged jets. After additional topological cuts, backgrounds are entirely dominated by physics backgrounds from $W \rightarrow Z b\bar{b}$, WZ and $t\bar{t}$. To improve the signal-to-background ratio further, the Higgs boson mass has to be reconstructed with the best possible resolution. Currently, a relative jet energy resolution of 13.9% has been achieved by DØ, as measured in Run II data for central jets at $E_T = 55 \text{ GeV}$. [4] It is expected that this can be improved by 30% due to more sophisticated jet reconstruction algorithms as well as refinements in jet energy calibration, including a calibration of the $b\bar{b}$ mass reconstruction using the $Z \rightarrow b\bar{b}$ signal.

A Higgs signal is then searched for as an excess in the $b\bar{b}$ mass spectrum, as shown in Fig. 1 for the CDF analysis. No evidence for WH production is observed in current Run II searches by CDF and DØ, allowing to set an upper limit on the product of cross-section and branching fraction $(\sigma_{WH}) \text{BR}(H \rightarrow b\bar{b})$ of 5 pb for a Higgs boson mass of 120 GeV, [5] which is still more than an order of magnitude higher than the Standard Model expectation.

In Fig. 2 the luminosity required to observe (or exclude) a Standard Model Higgs boson is shown as a function of mass. After combining all channels and both experiments, a sensitivity at the 95% C.L. for $m_H = 120 \text{ GeV}$ is expected to be achieved with an integrated luminosity of 1.8 fb^{-1} per experiment. Evidence for a signal at the 3 (5) level will require 4 fb^{-1} (10 fb^{-1}) for the same Higgs boson mass. These estimates assume a 30%

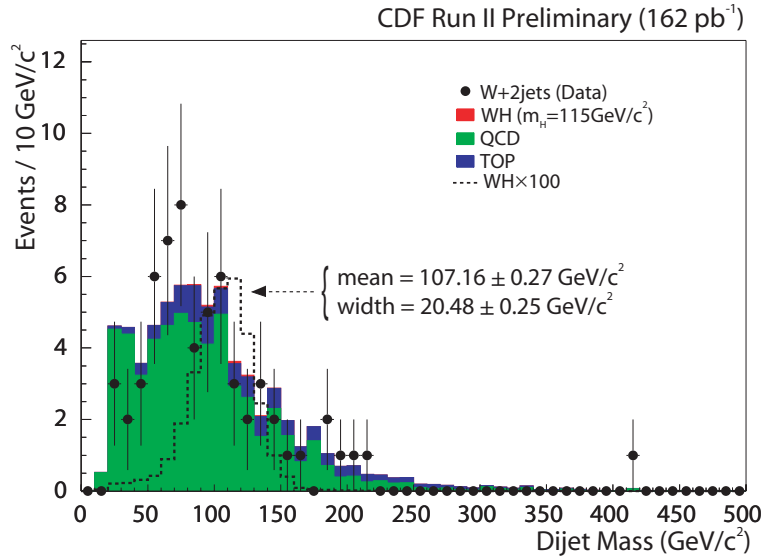


Figure 1: Invariant dijet mass spectrum in search for WH production in 162 pb^{-1} of CDF data in comparison with signal and background expectation.

improvement in jet energy resolution and do not include systematic errors. Given the Higgs event yields ($3 WH$ events selected per fb^{-1}), these analyses will require precise knowledge of the backgrounds over the entire mass range. While the normalization of the background can be obtained from a fit outside of the signal region, the shape and relative normalization of the dijet mass spectrum of the various background components has to be known to allow extrapolation below the Higgs peak. Procedures to obtain this information from data are outlined in Ref. [4] and typically involve a measurement of the shape of the dijet mass spectrum in background-enriched samples, which is then extrapolated to the signal sample using a mixture of Monte Carlo and data-driven methods.

3.2. $H \rightarrow WW$

Within the mass range of interest at the Tevatron, Higgs boson decays into two W bosons are the dominant decay mode for Higgs boson masses above 140 GeV . The relatively clean signature of two leptonic W decays allows to search for this decay in the gluon-gluon-fusion channel. While the production cross-section in this channel is higher compared to the associated production, the suppression due to the branching fractions of the leptonic W decays limits the event yield to only about 4 events per fb^{-1} .

Both Tevatron collaborations have started analyzing their Run II data in search for a $H \rightarrow WW$ signal [5]. So far, efficiencies of up to 15% (20% have been achieved for the dilepton plus B_t final states with electrons or muons). The background is dominated by WW production, which remains after selection cuts with a cross section of about 25 fb . Further separation of signal and WW events is possible using the difference in azimuthal angle between the two charged leptons. Due to spin correlations, $\Delta\phi$ tends to be small for decays of a spin-0 resonance. Both CDF and DØ observe no significant excess of events in 184 pb^{-1} and 176 pb^{-1} of Run II data, respectively. Limits on the production

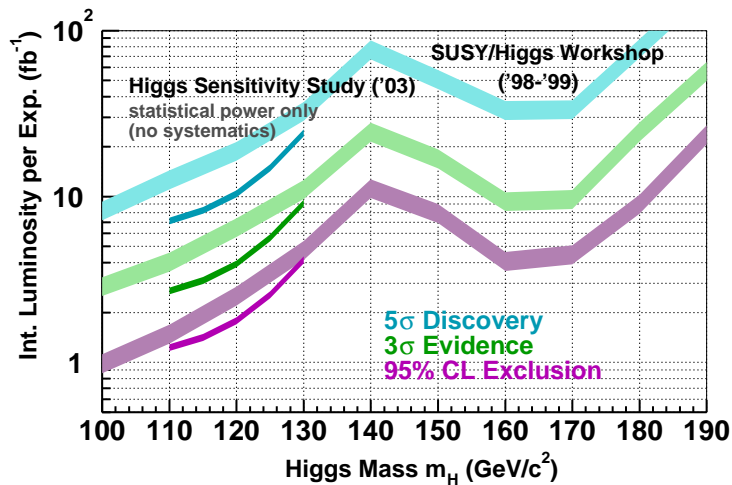


Figure 2: The integrated luminosity needed per experiment for a 95% CL exclusion, a 3 and a 5 discovery of a Standard Model Higgs boson at the Tevatron as a function of the Higgs boson mass, after combining all searches for associated production with a vector boson. Thin lines show recent estimates based on tuned full simulation [4], thick lines indicate results of an earlier study with fast simulation (includes searches for $H \rightarrow WW$). [3].

cross-section of $H \rightarrow WW$ have been set as a function of the Higgs boson mass as shown in Fig. 3. For a mass of 160 GeV, cross-sections larger than 5.6 pb have been excluded at 95% CL., which is still more than an order of magnitude higher than the expectation within the Standard Model.

The performance of these analyses is consistent with the expectations based on the fast simulation, which projected a total background of 30.4 fb at an efficiency of 18.5% for a Higgs boson mass of 150 GeV. [3] Based on this projection, sensitivity at the 95% CL. to a Standard Model Higgs boson with masses between 160 and 170 GeV will be reached with an integrated luminosity of 4 fb⁻¹ per experiment (10 fb⁻¹ for a 3 sensitivity), as shown in Fig 2.

In models beyond the Standard Model, the rate of $H \rightarrow WW$ events can be enhanced due to larger production cross-sections (models with heavy 4th generation quarks) or due to an increase in branching fraction (Topcolor models [3]). In the former case, the gluon-gluon fusion process is enhanced due to loop-diagrams involving heavy quarks by a factor of about 8.5 within the mass range of interest at the Tevatron, with only a mild dependence on the heavy quark mass. [7] The latter class of models also predicts an enhanced branching fraction for $H \rightarrow \gamma\gamma$, which can be searched for with diphoton analyses to increase the Tevatron sensitivity at low Higgs boson masses. [3] First Run II results from D in this channel exist, but improve only marginally on existing limits from LEP and Run I. [8]

3.3. Neutral Higgs Bosons in Supersymmetry

Sensitivity to a low-mass Higgs boson is of particular interest within supersymmetric

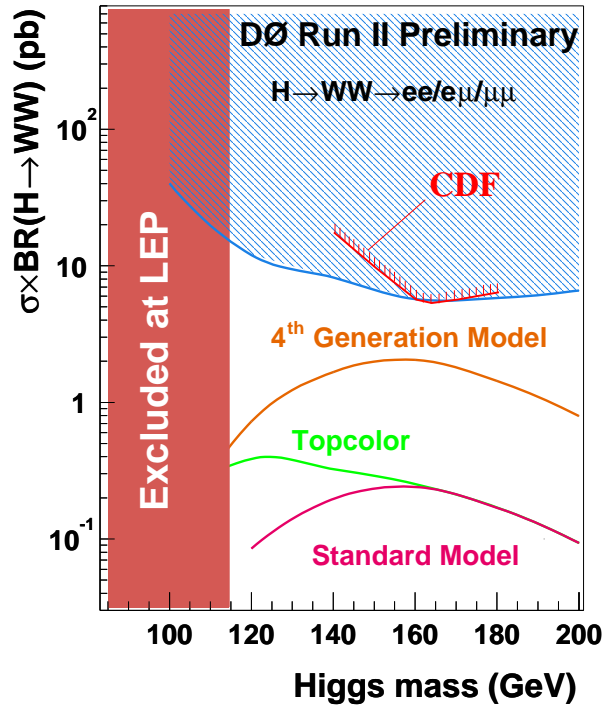


Figure 3: Upper limit (at 95% CL) on the cross section $\sigma \times \text{BR}(H \rightarrow WW)$ set by the DØ Collaboration using 176 pb^{-1} of Run II data, modified to include the limit set by the CDF Collaboration using 184 pb^{-1} of Run II data. The limits are compared to expectations from Standard Model Higgs production and alternative models.

extensions of the Standard Model, which predict the existence of at least one neutral Higgs boson $= h; H; A$ with a mass below 135 GeV . Searches for the Standard Model Higgs boson produced in association with a vector boson can be interpreted within SUSY parameter space. In addition, the enhancement of the Higgs coupling to bb at large $\tan\beta$ results in sizeable cross-sections for two search channels that are inaccessible within the Standard Model: the production of Higgs bosons in association with one or more b -quarks[9] as well as the gluon-gluon-fusion channel $gg \rightarrow H$ with the subsequent decay $H \rightarrow bb$.

3.3.1. $b(b) \rightarrow bb(b)$

The DØ collaboration has analyzed 131 pb^{-1} of Run II data collected with multijet triggers optimized for the $bb \rightarrow bb(b)$ signal.[6] Requiring two jets with transverse momenta $p_T > 25 \text{ GeV}$ and a third jet with $p_T > 15 \text{ GeV}$, this trigger consumed less than 4 Hz of Level-3 bandwidth at instantaneous luminosities of $4.0 \times 10^3 \text{ cm}^{-2} \text{ s}^{-1}$, while maintaining a signal efficiency of about 70% after online cuts. The offline analysis requires at least three b -tagged jets with $p_T > 15 \text{ GeV}$. Depending on the Higgs mass hypothesis, the p_T cuts for the leading two jets are tightened to values between 35 and 60 GeV to optimize for best expected sensitivity.

The background at this stage is dominated by multijet production with b-quarks. Further discrimination is possible by searching for a peak in the invariant mass spectrum of the two leading jets, which is shown in Fig. 4 in comparison with the expectation from

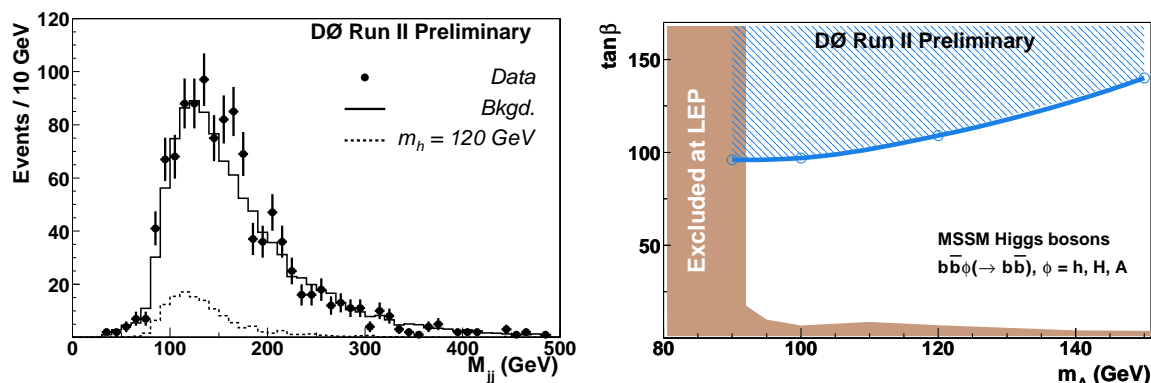


Figure 4: Invariant mass spectrum of the two leading jets in the 3-jet sample with three b-tags after final cuts in the D^0 search for $b\bar{h}$ production using 131 pb^{-1} of Run II data (left); Regions in $(\tan \beta, m_A)$ excluded by this analysis at 95% C.L. in comparison with LEP limits (right).

background and a Higgs signal with $m_h = 120 \text{ GeV}$. The shape of the dijet mass spectrum in background is obtained from a multijet sample with two b-tagged jets, which is expected to have negligible contamination from signal, by weighting events using b-tag fake rates measured in data as a function of jet p_T and η . The background is then normalized by fitting this shape to the mass spectrum outside the signal region.

No evidence for production of neutral Higgs bosons h, H, A in association with b-jets has been observed, which allows to derive limits on $\tan \beta$ as a function of m_A . In Fig. 4 the region excluded in the plane of $(\tan \beta, m_A)$ is shown in comparison with existing limits set by the LEP experiments. The D^0 Run II limit is significantly worse than the limit published in 2001 by the CDF collaboration based on the analysis of 91 pb^{-1} of Run I data. [10] Detailed comparisons of both results indicate that the apparent loss of sensitivity observed by D^0 can be traced back to the use of more recent cross-section calculations and PDFs, which cause a significant reduction in signal acceptance and cross-section compared to the CDF Run I analysis. [11]

With more luminosity and after combining results from both Tevatron experiments, the reach in $\tan \beta$ at the 95% C.L. will be extended to about $\tan \beta = 25$ at $m_A = 120 \text{ GeV}$ (for 5 fb^{-1} , within the mhm ax scenario [12]), but deteriorates quickly with increasing m_A .

3.3.2. $b\bar{h}$

In addition to the usually dominant decay mode $b\bar{h}$, a light supersymmetric Higgs boson can be searched for in its decay to $b\bar{b}$. This decay mode is of particular interest both for SUSY scenarios that favour suppressed couplings of Higgs bosons to b-quarks as well as for the large $\tan \beta$ region, where the channels $b(b) \rightarrow b(b)$ and $gg \rightarrow b\bar{b}$ provide a viable complement to the search for $b(b) \rightarrow b\bar{b}(b)$.

Both Tevatron experiments have demonstrated the ability to reconstruct hadronic tau decays in Run II data by measuring the $Z \rightarrow \tau\tau$ cross-section. The CDF collaboration has analyzed 200 pb⁻¹ of Run II data in search for $gg \rightarrow H \rightarrow \tau\tau$ with one tau decaying leptonically to electron or muon and the other tau decaying into hadrons.[6] The hadronic tau decay is reconstructed as one or more tracks pointing to a narrow energy deposition in the calorimeter. Background from jets misreconstructed as tau objects is further suppressed using cuts on track multiplicity, mass and isolation of the tau candidate. The selection then requires one such tau candidate in addition to an isolated electron or muon. After topological cuts using the transverse momenta of the lepton, the tau candidate as well as the transverse missing energy, the sample is dominated by irreducible background from $Z \rightarrow \tau\tau$ with a purity of 90%. Higgs events are selected with an efficiency of about 7% (5%) in the electron (muon) channel.

Separation of signal events from the $Z \rightarrow \tau\tau$ background is possible by reconstructing an event mass m_{vis} based on the momenta of lepton and tau candidate as well as the missing transverse energy. Fig. 5a shows the distribution of m_{vis} for data, backgrounds and

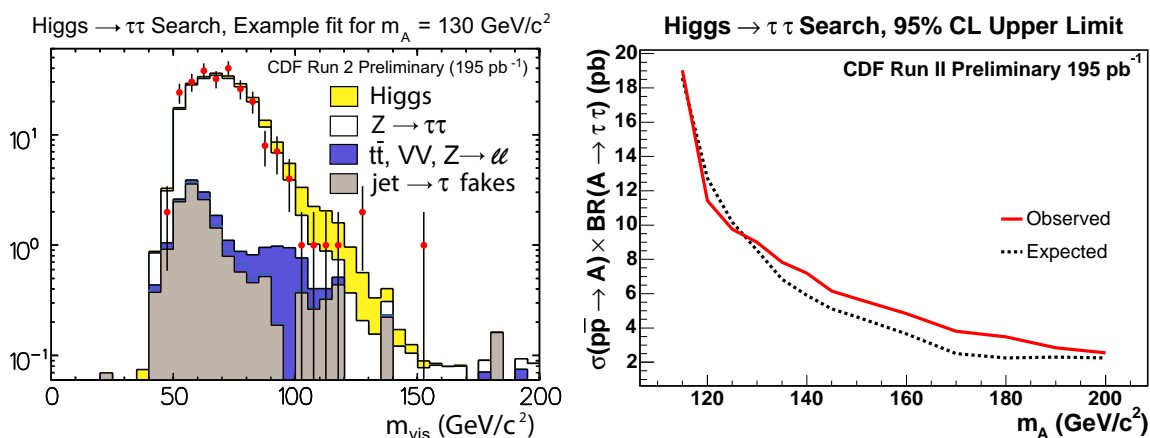


Figure 5: Distribution of visible mass after all cuts of the CDF search for $H \rightarrow \tau\tau$ in 195 pb⁻¹ of Run II data (left); Upper limit (at 95% CL) on the cross-section $\sigma(pp \rightarrow H) \times BR(H \rightarrow \tau\tau)$ in comparison with the expected limit (right).

a potential Higgs signal. No evidence for an excess of events with respect to the Standard Model prediction has been observed. Using a binned likelihood fit of this distribution, a limit on the production cross-section of $gg \rightarrow H$ has been extracted as displayed in Fig. 5b as a function of the Higgs boson mass.

3.3.3. Combined Reach

Combining dedicated searches for Higgs bosons at high $\tan \beta$ with searches for production of Higgs bosons in association with vector bosons, sensitivity at 95% CL to MSSM Higgs bosons within the mhmax scenario can be achieved independent of $\tan \beta$ with 5 fb⁻¹ per experiment, as shown in Fig. 6.[3] However, within this challenging scenario, a 5 discovery will not be possible at Tevatron Run II for most of the $(\tan \beta, m_A)$ plane.

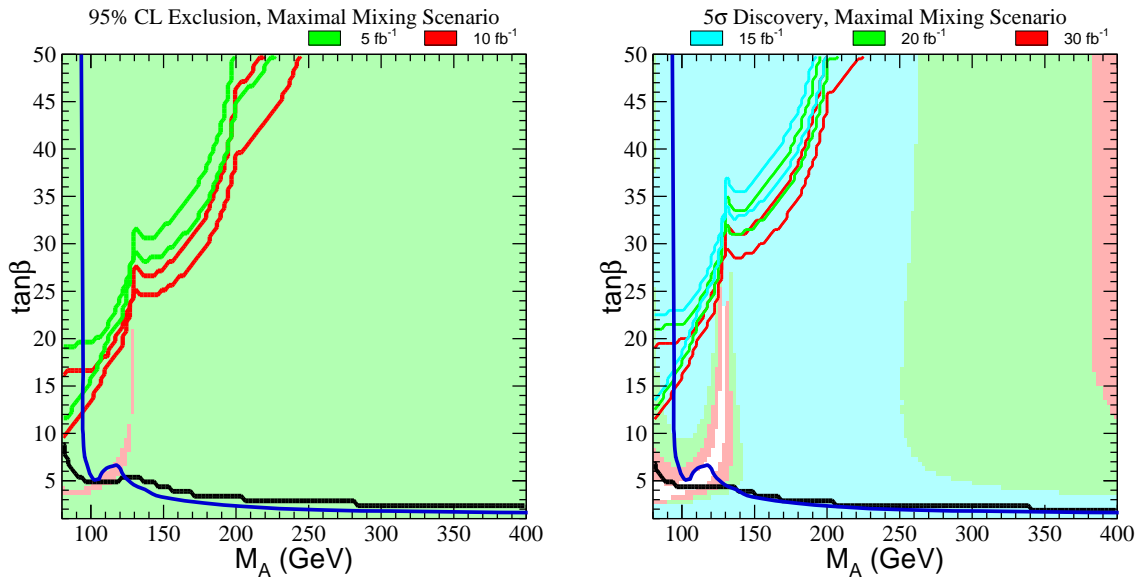


Figure 6: Luminosity required for exclusion at 95% C.L. (left) or 5 σ discovery (right) of a SUSY Higgs boson as a function of m_A and $\tan\beta$ within the m_{hmax} scenario (taken from Ref. [3] and modified to include most recent LEP 2 limit [13]). Shaded regions indicate the reach of $W H / Z H$ searches, the region above the diagonal lines are accessible to searches for $h b(\bar{b})$, the dark line indicates the LEP 2 limit.

3.4. Charged Higgs Bosons

Models with an extended Higgs sector predict charged Higgs bosons H^\pm , or in the case of additional Higgs Triplets doubly-charged Higgs bosons $H^{\pm\pm}$. Production of doubly charged Higgs bosons can provide particularly striking signatures in LR inspired models, where $\text{BR}(H^{\pm\pm} \rightarrow \ell^+\ell^-)$ is expected to be 100%. CDF (D) have analyzed 240 pb^{-1} (107 pb^{-1}) of Run II data to search for $H^{\pm\pm}$ production in like-sign dilepton events.[6] Requiring two acoplanar, isolated electrons or muons, no excess of events has been observed at high dilepton masses. For left-handed (right-handed) $H^{\pm\pm}$, CDF set a lower mass limit of 135 GeV (112 GeV) for $\text{BR}(H^{\pm\pm} \rightarrow \ell^+\ell^-) = 1$.

4. Searches for Supersymmetry

Supersymmetry predicts a large number of new particles, most of which could be light enough to be produced at the Tevatron. The CDF and D collaborations have searched their Run II data for evidence of squarks, gluinos, charginos and neutralinos. For most analyses, minimal Supergravity (mSUGRA) is used as a reference model for optimization of the analysis and interpretation of the result, even though the resulting cross-section limits can be interpreted in a more model-independent way. Alternative models leading to different final state topologies have been considered as well, including models with gauge-mediated SUSY breaking as well as R-parity violation.

The following sections summarize a selection of current Tevatron results with relevance

to Supersymmetry.

4.1. Squarks and Gluinos

Squarks and gluinos are produced through the strong interaction, resulting in relatively large signal cross-sections and therefore providing, if kinematically accessible, a promising signature for Supersymmetry at the Tevatron. The final state contains two or more jets along with missing transverse energy carried away by the two lightest supersymmetric particles. DØ have searched for pair production of squarks, each decaying into a quark and the lightest neutralino.[14] This decay channel is expected to be dominant if the gluino is heavier than the squark. 85 pb⁻¹ of Run II data collected with a dedicated multijet trigger have been analyzed using tight cuts on $\cancel{E}_T > 175$ GeV and $H_T > 275$ GeV against the massive multijet background. Fig. 7a shows the \cancel{E}_T distribution after all other cuts, with a tail at high \cancel{E}_T expected from standard model processes such as Z + jets with Z → $\nu\bar{\nu}$.

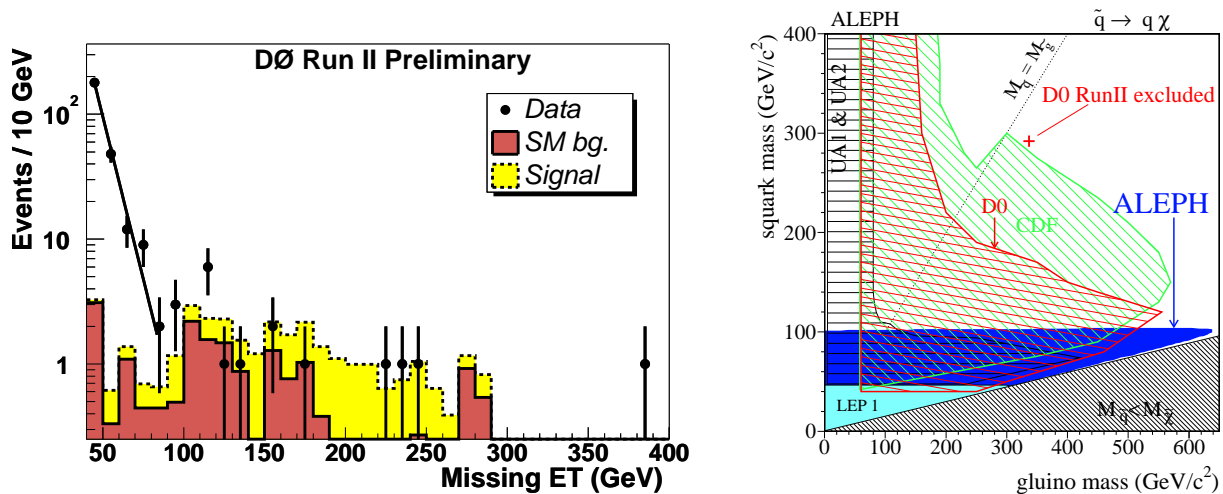


Figure 7: Distribution of \cancel{E}_T after all cuts except for the cut on \cancel{E}_T itself (left), showing contributions from multijet backgrounds (line), other standard model processes (red) and signal (yellow); point in the squark/gluino mass plane corresponding to the limit set by the DØ analysis for the mSUGRA model line with $m_0 = 25$ GeV, $\tan\beta = 3$, $A_0 = 0$ and $\mu < 0$ (right).

After a veto of events containing isolated leptons to suppress background from leptonic W decays, an expectation of 2.7 ± 1.0 Standard Model events remains. Four events are observed in the DØ data, allowing to set upper limits on the squark production cross-section of about 2 pb. Assuming that squarks are degenerate in mass for the first two generations, the reach in mSUGRA parameter space has been evaluated for $m_0 = 25$ GeV, $\tan\beta = 3$, $A_0 = 0$ and $\mu < 0$ (see Fig. 7). For this model line, squark masses below 292 GeV can be excluded, corresponding to a slight improvement over existing limits (see Fig. 7b).

For the third generation, mass unification is broken in many SUSY models due to potentially large mixing effects. This can result in third generation squarks much lighter than the other squarks and the gluino. The CDF collaboration has considered this scenario by searching 156 pb⁻¹ of Run II data for pair production of gluinos which subsequently decay to b-quarks plus sbottoms, resulting in final states with four b-quarks and missing

transverse energy. [15] Signal events are isolated by requiring the presence of at least three jets with $E_T > 15 \text{ GeV}$, one or two of which need to be b-tagged using a secondary vertex algorithm. After an additional cut on $E_T > 80 \text{ GeV}$, 2.6 ± 0.7 events are expected from Standard Model sources, while four events are observed in the data. Assuming a gluino branching fraction to sbottoms of 100%, regions in the gluino/sbottom mass plane can be excluded up to gluino masses of 280 GeV (see Fig. 8).

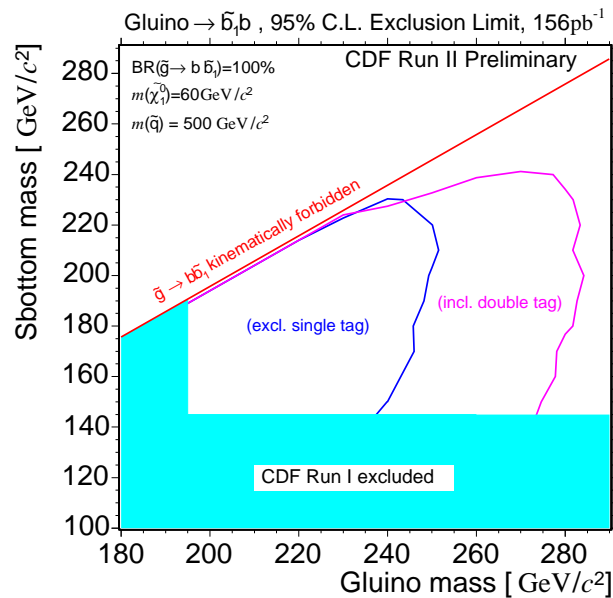


Figure 8: Regions in the gluino/sbottom mass plane excluded by the CDF Run II analysis requiring one (blue line) or two (violet line) b-tagged jets.

CDF also considered a scenario with light stop quarks, in this case assuming that stops are long-lived and decay outside of the detector. [16] Experimentally, pair production of light stable stop quarks can be detected as a pair of heavily ionizing, slow moving charged particles. The events are triggered on using standard muon triggers, and then selected in offline analysis using the time-of-flight detector. In this way backgrounds from light particles are suppressed to an expectation of 2.9 ± 0.7 (stat) ± 3.1 (syst) in 53 pb^{-1} of Run II data. Seven events have been observed, allowing to exclude stop masses below 107 GeV (95 GeV) for isolated (non-isolated) stops.

4.2. Charginos and Neutralinos

Many SUSY models expect squarks and gluinos to be the heaviest supersymmetric particles, which might well put them out of the reach of the Tevatron Run II experiments. In this case, a search for the associated production of charginos and neutralinos provides the most promising way for direct detection of supersymmetric particles at the Tevatron. Due to its striking signature, the trilepton channel $e^+ \tilde{\chi}_2^0 + \tilde{\chi}_1^+ + \tilde{\chi}_1^0 \tilde{\chi}_1^0$ is considered the most powerful analysis channel, despite its low rate due to the small cross-section and branching fraction. The D collaboration has searched for an excess of trilepton events in 175 pb^{-1} of Run II data. [17] Three different selections have been defined to cover

topologies with two electrons and a third isolated track, one electron plus one muon with a third isolated track, and two muons with the same charge. To maintain the highest-possible efficiency, the third lepton is reconstructed (if at all) as an isolated track, which is designed to be efficient for electrons, muons and hadronic tau decays. A total of 0.9 events are expected from Standard Model backgrounds, dominated by irreducible backgrounds from W^+W^- and WZ as well as W with a converted photon. Two events are observed in data, allowing to set an upper limit of about 0.6 pb on production cross-section times branching fraction into three leptons. Fig. 9 shows this limit as a function of the chargino mass in comparison with the LEP limit from direct chargino searches. The new DØ limit significantly improves on the Run I limit, but for signal rates as expected within minimal SUGRA is not yet sensitive to chargino masses beyond the LEP limit.

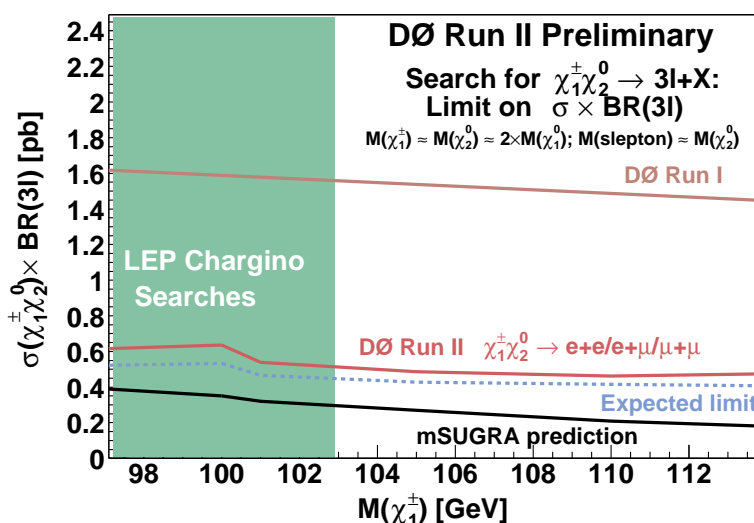


Figure 9: The DØ Run II limit (red line) and expected limit (dashed line) on cross-section times branching fraction into three leptons from the search for associated chargino/neutralino production. The shaded area is excluded by direct chargino searches at LEP, the black line shows the expectation within mSUGRA for slepton masses equal to the second lightest neutralino mass.

4.3. $B_s \rightarrow \mu^+ \mu^-$

While not a direct search for supersymmetric particles, the measurement of the branching fraction of $B_s \rightarrow \mu^+ \mu^-$ is a sensitive probe of Supersymmetry. This rare flavour-changing neutral current decay is heavily suppressed within the Standard Model, where a branching fraction of only 3.8×10^{-9} is expected. However, within supersymmetry this decay can be significantly enhanced by loop corrections. For instance, within SUGRA the branching fraction is proportional to $(\tan \beta)^6$, leading to an enhancement of up to three orders of magnitude.[18] At the Tevatron, B_s mesons are produced with a very large rate, and a possible decay into two muons can be identified with high efficiency. Both collaborations have reported on analyses searching about 170 pb^{-1} of Run II data for evidence of this rare decay. The selection suppresses dimuon background from prompt production and semi-leptonic b-decays by requiring two isolated muons originating from a vertex

that is significantly displaced from the primary interaction point. Both CDF and DØ estimate the sensitivity of their analysis to branching fractions of about $9 \cdot 10^{-7}$ at 95% C.L.[19] While DØ have not yet quoted a result, CDF observe no significant excess of events in the search window around the B_s mass (see Fig. 10) and have set a limit of $BR(B_s \rightarrow \mu^+\mu^-) < 7.5 \cdot 10^{-7}$ at 95% C.L.

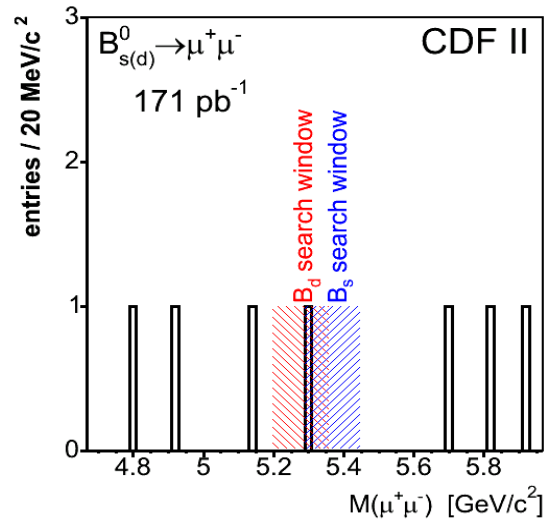


Figure 10: Dimuon invariant mass distribution after all cuts of the CDF Search for $B_s \rightarrow \mu^+\mu^-$. One event is found in the B_s search window, consistent with the background expectation extrapolated from the side bands.

4.4. Gauge-Mediated SUSY Breaking

The mass hierarchies expected in models with gauge-mediated SUSY breaking (GMSB) can significantly alter the signatures of supersymmetry at colliders. While the gravitino is expected to be the lightest supersymmetric particle in these models, the NLSP can be either a neutralino or a slepton. Neutralino NLSPs decay to a photon and a gravitino, the latter escaping detection in a collider detector. Production of charginos and neutralinos therefore leads to final states containing at least two photons and missing transverse energy. Both Tevatron collaborations have searched for an excess of such events in about 200 pb^{-1} of Run II data.[20] After requiring missing transverse energy larger than 40 GeV (45 GeV), DØ (CDF) observe one (zero) events compared to an expected background of 2.5 ± 0.5 (0.6 ± 0.5) events. Limits on the production cross-section of charginos and neutralinos have been set as a function of chargino mass (see Fig. 11). Within a particular GMSB scenario (one messenger field, $M = 2$, $\tan \beta = 5$, $\mu > 0$), these limits can be translated into lower limits on chargino (neutralino) masses of 192 GeV (105 GeV) and 168 GeV (93 GeV) for DØ and CDF, respectively.

5. Other Searches for New Physics

A large variety of other searches have been performed at the Tevatron. While not

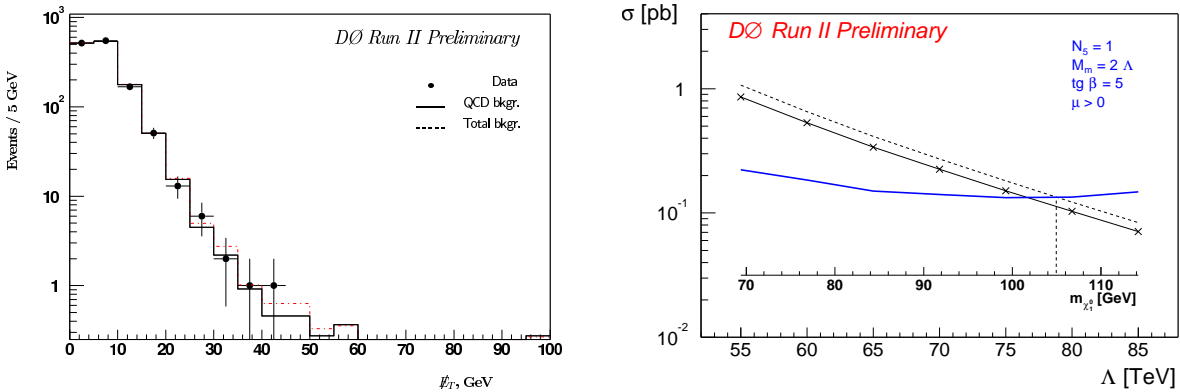


Figure 11: The distribution of missing transverse energy (left) after all cuts of the D search for GM SB SUSY, compared to the expectation within the Standard Model (dashed line) and the prediction for multi-jet events (solid line); Upper cross-section limit on GM SB SUSY with neutralino NLSP in comparison with the NLO signal cross-section (right).

directly aimed at the discovery of supersymmetric particles, most of the topologies covered by these searches are of relevance for SUSY models as well. This section gives a brief overview of these results.

Final states with two high- p_T leptons or photons are predicted in a number of extensions of the Standard Model. Signals include new neutral gauge bosons Z^0 as well as the production or exchange of gravitons in models with extra dimensions. Both CDF and D have observed no significant excess in their high- p_T dilepton and diphoton data, as demonstrated by the good agreement between data and background predictions in the invariant dilepton mass distributions shown in Fig. 12. For given models, these results

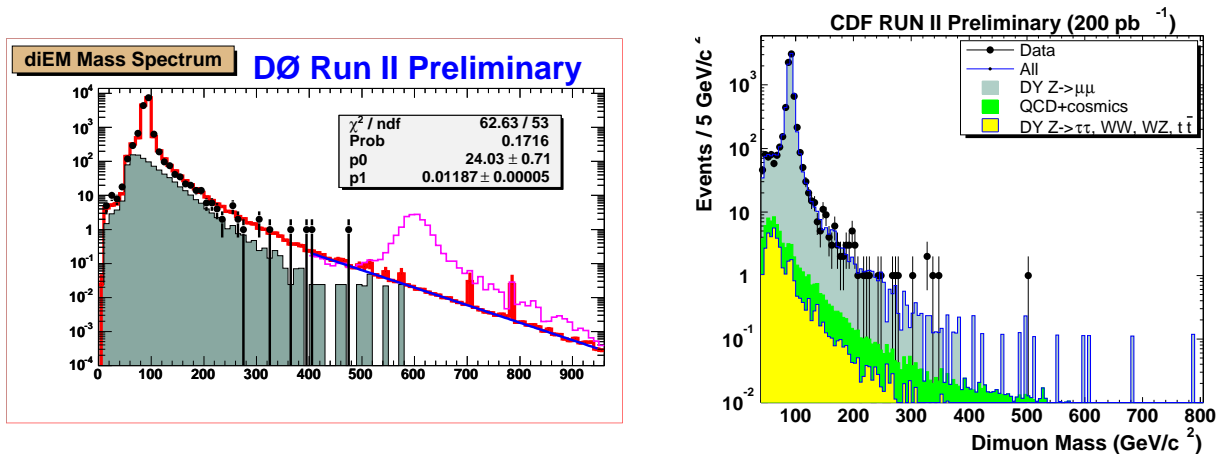


Figure 12: Distribution of invariant dielectron (left) and dimuon (right) mass in the high- p_T dilepton searches by D and CDF, respectively. The left plot shows the MC expectation for a Z^0 signal with $m_{Z^0} = 600$ GeV on top of the Standard Model backgrounds.

can be translated into limits on Z^0 masses or the fundamental Planck scale as summarized in Table 1.[21]

Table 1: Selection of most stringent CDF and D limits on dilepton resonances, leptoquarks, excited leptons and large extra dimensions. The results are quoted for (1) a sequential Z^0 with Standard Model couplings, (2) scalar leptoquarks with 100% branching fraction, (3) a contact interaction scale equal to the mass of the excited electron, (4) the GRW convention, (5) four extra dimensions.

Analysis	Channel	Limit	
High-mass Dilepton	D, 200 pb ⁻¹	$Z^0 \rightarrow ee$	$m_{Z^0} > 780 \text{ GeV}^{(1)}$
	CDF, 200 pb ⁻¹	$Z^0 \rightarrow \mu\mu$	$m_{Z^0} > 735 \text{ GeV}^{(1)}$
	CDF, 195 pb ⁻¹	$Z^0 \rightarrow \tau\tau$	$m_{Z^0} > 394 \text{ GeV}^{(1)}$
Leptoquarks	D, 175 pb ⁻¹	$LQ \rightarrow eq$	$m_{LQ} > 240 \text{ GeV}^{(2)}$
	CDF, 198 pb ⁻¹	$LQ \rightarrow q\bar{q}$	$m_{LQ} > 241 \text{ GeV}^{(2)}$
	CDF, 191 pb ⁻¹	$LQ \rightarrow q\bar{q}$	$m_{LQ} > 117 \text{ GeV}^{(2)}$
Excited Electrons	CDF, 200 pb ⁻¹	$e \rightarrow e$	$m_e > 889 \text{ GeV}^{(3)}$
Large Extra Dimensions	D, 200 pb ⁻¹	$\mu\mu, ee$	$M_S > 1.43 \text{ TeV}^{(4)}$
	D, 85 pb ⁻¹	$\text{jet} + G_{KK}$	$M_D > 685 \text{ GeV}^{(5)}$

Similar searches exist for other new high-mass particles such as leptoquarks [22], 4th generation quarks [23] and excited leptons [24]. Given the high mass scale of the signal, fairly stringent cuts on transverse energy can be applied to select final states with high- p_T jets, leptons or large missing transverse energy. No evidence for any excess has been reported. Table 1 summarizes the mass limits that have been derived by CDF and D.

6. Acknowledgements

I would like to thank my colleagues at CDF and D for providing the material for this presentation as well as the organizers of the SUSY 2004 conference for this very well-organized event.

7. References

- [1] CDF Collaboration, The CDF II Detector Technical Design Report, FERMILAB-Pub-96/390-E.
- [2] D Collaboration, The Upgraded D Detector, to be submitted to Nucl. Instrum. Methods A; T. LeCompte and H.T. Diehl, Ann. Rev. Nucl. Part. Sci. 50, 71 (2000).
- [3] M. Carena, J.S. Conway, H.E. Haber et al., Report of the Higgs working group of the Tevatron Run II SUSY/Higgs workshop, hep-ph/0010338.
- [4] CDF and D Collaborations, Results of the Tevatron Higgs Sensitivity Study, FERMILAB-PUB-03/320-E (2003).
- [5] J. Conway, Search for the Standard Model Higgs in Run 2 at the Tevatron, these proceedings; G. Davies, Standard Model Higgs Searches at D, these proceedings.
- [6] A. Anastassov, Search for new phenomena with tau pairs, these proceedings; A. Turcot, Non-Standard Model Higgs Searches at D, these proceedings.

- [7] E. Arık, M. Arık, S.A. Cetin, T. Conka, A. Mailyov and S. Sultansoy, Eur. Phys. J. C 26 (2002) 9.
- [8] D Collaboration, Search for non-SM Light Higgs Boson in the $h \rightarrow \tau^+ \tau^-$ Channel at D in Run II, D Note 4374-CONF.
- [9] J. Campbell, R.K. Ellis, F. Maltoni, S. Willenbrock, Phys. Rev. D 67 (2003) 095002, hep-ph/0204093 v2.
- [10] CDF Collaboration, Phys.Rev.Lett. 86 (2001) 4472.
- [11] J. Yamamoto, Uncertainties on PDF's affecting 3b/4b MSSM Higgs search, Presentation at the Tev4LHC Workshop, Fermilab, Sep 16, 2004.
- [12] M. Carena, S. Heinemeyer, C.E. Wagner and G. Weiglein, Eur. Phys. J. C 26, (2003) 601.
- [13] The ALEPH, DELPHI, L3 and OPAL collaborations and the LEP Higgs working group, CERN-EP/2001-055, hep-ex/0107030.
- [14] J. Yu, Searches for Squark, Gluino, and LED in MET + Jets Topology at D, these proceedings.
- [15] C. Rott, Searches for the Supersymmetric Partner of the Bottom Quark, these proceedings.
- [16] CDF Collaboration, Search for stable Stop Quarks, <http://www-cdf.fnal.gov/physics/exotic/run2/champs-2003/champs-public.html>
- [17] J. Butler, Search for SUSY in the multilepton final states, these proceedings.
- [18] A. Dedes, H.K. Dreiner, U. Nierste, P. Richardson, Trilepton Events and $B_s \rightarrow \tau^+ \tau^-$: No-lose for mSUGRA at the Tevatron?, hep-ph/0207026, and references therein.
- [19] CDF Collaboration, A Search for $B_{s(d)}^0 \rightarrow \tau^+ \tau^-$ Decays at CDF, CDF Note 6397; D Collaboration, Sensitivity Analysis of the rare decay $B_s \rightarrow \tau^+ \tau^-$ with the D detector, D Note 4377-CONF.
- [20] Y. Coadou, Search for GMSB SUSY in diphoton events with large missing ET, these proceedings.
- [21] E. Gallas, Searches for Extra Dimensions and Heavy di-lepton Resonances at D, these proceedings; T. P. Rat, CDF Searches for New Physics at High Diphoton and Dilepton Masses, these proceedings.
- [22] R. Strohmeyer, Searches for Leptoquarks, these proceedings.
- [23] R. Erbacher, Searches for New Physics in the Top Quark Sample, these proceedings.
- [24] CDF Collaboration, Search for Excited and Exotic Electrons in the $e^+ e^-$ Channel, CDF Note 7177.